

*Supporting Information*

**Nanoscale Polarization Switching and Magneto–Piezoelectric Coupling in MgFe<sub>2</sub>O<sub>4</sub>–  
PVDF-HFP Nanocomposites for Low-Field Magnetic Energy Harvesting and Self-  
Powered IoT Microsystems**

*B. Sheetal Priyadarshini*<sup>1,2</sup>, *Dhiman Kalita*<sup>3</sup>, *Nevin Noble*<sup>4,5</sup>, *Giorgio Bais*<sup>6</sup>, *Dinesh  
Topwal*<sup>4,5</sup> and *Unnikrishnan Manju*<sup>1,2</sup> \*

<sup>1</sup> *Materials Chemistry and Interfacial Engineering Department, CSIR-Institute of Minerals  
and Materials Technology, Bhubaneswar, Odisha 751013, India*

<sup>2</sup> *Academy of Scientific and Innovative Research (AcSIR), Ghaziabad, Uttar Pradesh  
201002, India*

<sup>3</sup> *School of Engineering, RMIT University, 124 La Trobe Street, Melbourne, Victoria, 3001  
Australia*

<sup>4</sup> *Institute of Physics, Sachivalaya Marg, Bhubaneswar 751005, India*

<sup>5</sup> *Homi Bhabha National Institute, Training School Complex, Anushakti Nagar, Mumbai  
400085, India*

<sup>6</sup> *Elettra- Sincrotrone Trieste, Trieste 34149, Italy*

*Corresponding author: [manju.immt@csir.res.in](mailto:manju.immt@csir.res.in)*

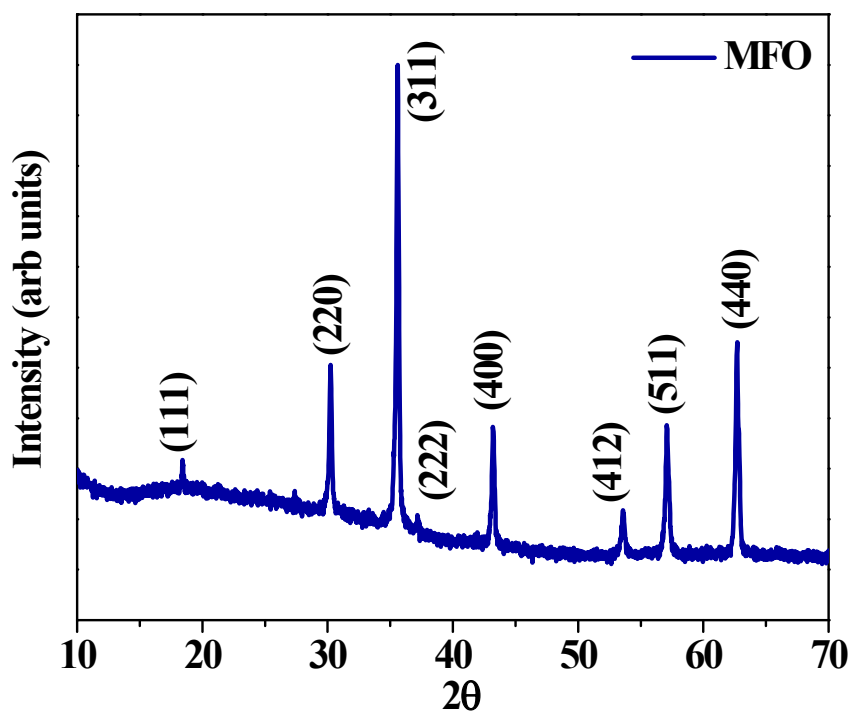


Figure S1: Room temperature x-ray diffraction pattern of  $\text{MgFe}_2\text{O}_4$

Table S1: Crystallographic data of  $\text{MgFe}_2\text{O}_4$  at 900 °C.

<b>Crystal system</b>	<b>Cubic</b>
<b>Space group</b>	$Fd\bar{3}m$
<b>Unit cell dimension</b>	$a=b=c= 8.47224 (9) \text{ \AA}$
	$\alpha= \beta= \gamma= 90^\circ$
<b>Atomic Coordinates</b>	
<b>O</b>	(0.25472, 0.25472, 0.25472)
<b>MgT</b>	(0.125, 0.125, 0.125)
<b>FeT</b>	(0.125, 0.125, 0.125)
<b>MgO</b>	(0.5, 0.5, 0.5)
<b>FeO</b>	(0.5, 0.5, 0.5)
$\chi^2$	5.89
$R_p$	5.79%
$R_{wp}$	5.49%

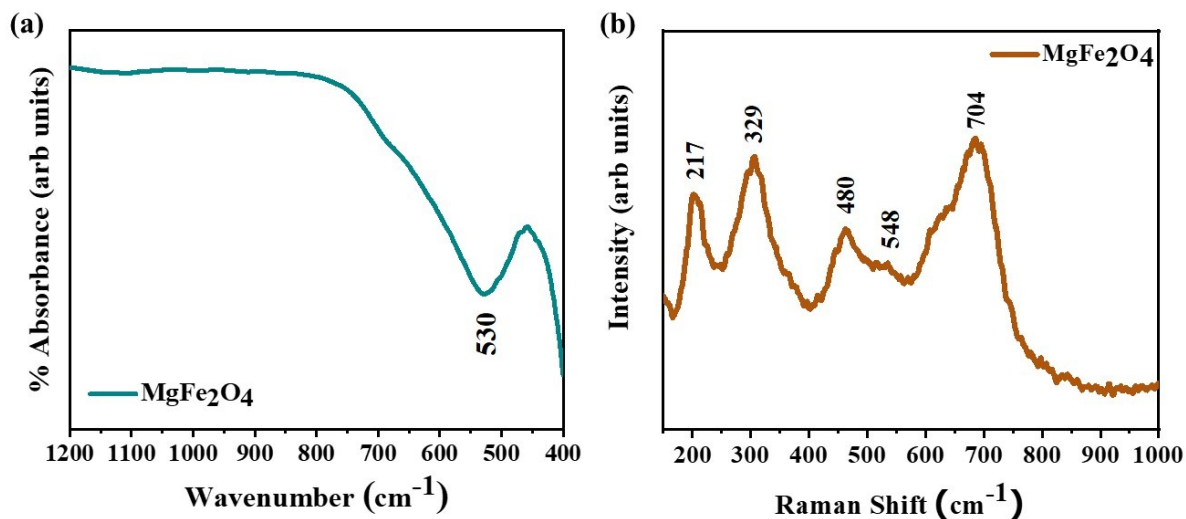


Figure S2: (a) Fourier transform infrared spectroscopy and (b) Raman spectroscopy data of MgFe<sub>2</sub>O<sub>4</sub> at room temperature.

Figure S2a shows the obtained FT-IR spectrum of MFO in the wavenumber range from 400 to 1200 cm<sup>-1</sup>. The strong absorption band at ~530 cm<sup>-1</sup> indicates the formation of MFO, which can be assigned to the metal-oxygen band corresponding to the intrinsic stretching vibrations of the metal at the tetrahedral site<sup>1</sup>. The vibrational and structural properties of MFO are further probed with Raman spectroscopy, shown in Figure S2b. MgFe<sub>2</sub>O<sub>4</sub> spinel structure consists of five Raman active modes assigned as one A<sub>1g</sub>, one E<sub>g</sub>, and three F<sub>2g</sub> modes<sup>2</sup>. The F<sub>2g</sub> mode at 217 cm<sup>-1</sup> is due to translational movement of the whole tetrahedron (FeO<sub>4</sub>). Raman mode at 329 cm<sup>-1</sup>, which can be assigned to E<sub>g</sub>, is due to the symmetric bending of oxygen with respect to Fe. Raman modes at 480 and 548 cm<sup>-1</sup> are assigned to F<sub>2g</sub> which are related to the vibrations of the octahedral group. The 480 and 548 cm<sup>-1</sup> modes are caused by the asymmetric stretching and bending of the Fe-O bond, respectively. The A<sub>1g</sub> mode at 704 cm<sup>-1</sup> corresponds to the symmetric stretching of oxygen atoms along Fe-O tetrahedral bonds.

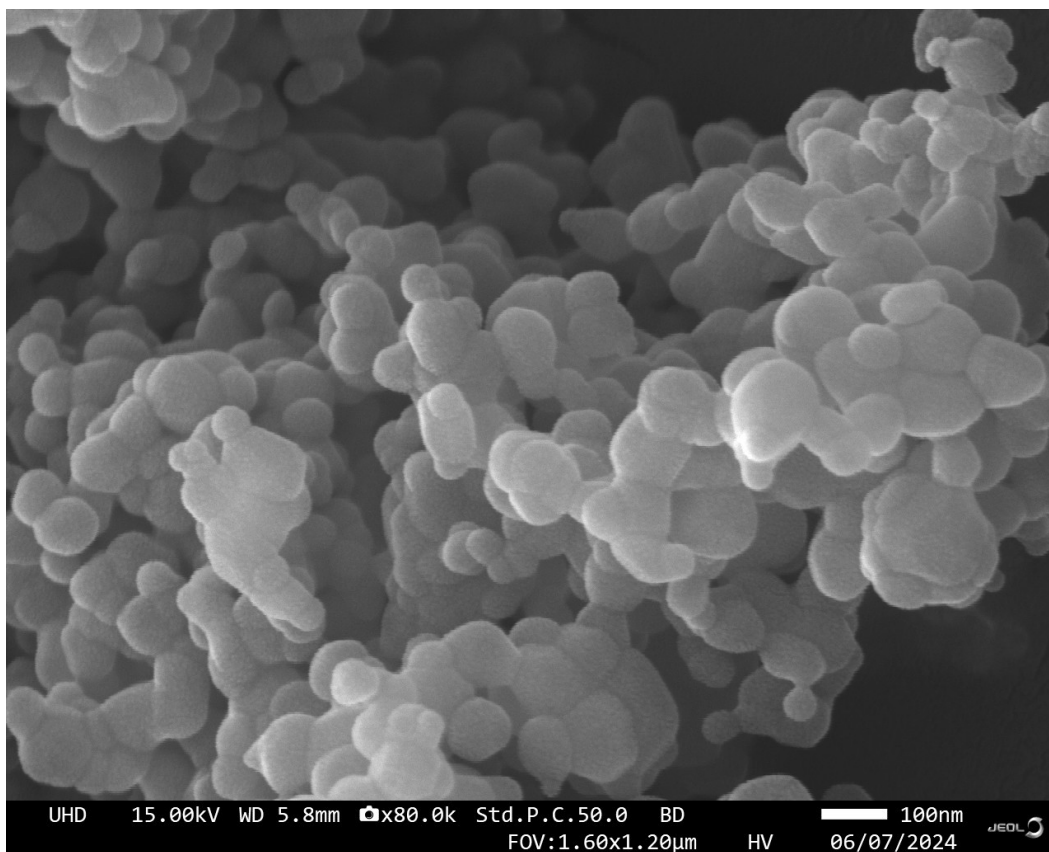


Figure S3: Scanning electron microscopy image of  $\text{MgFe}_2\text{O}_4$  nanoparticle synthesized via the sol-gel method.

The SEM image of the as-synthesized MFO nanoparticles is shown in Figure S3. The average particle size of the nanoparticle is found to be 69.4 nm.

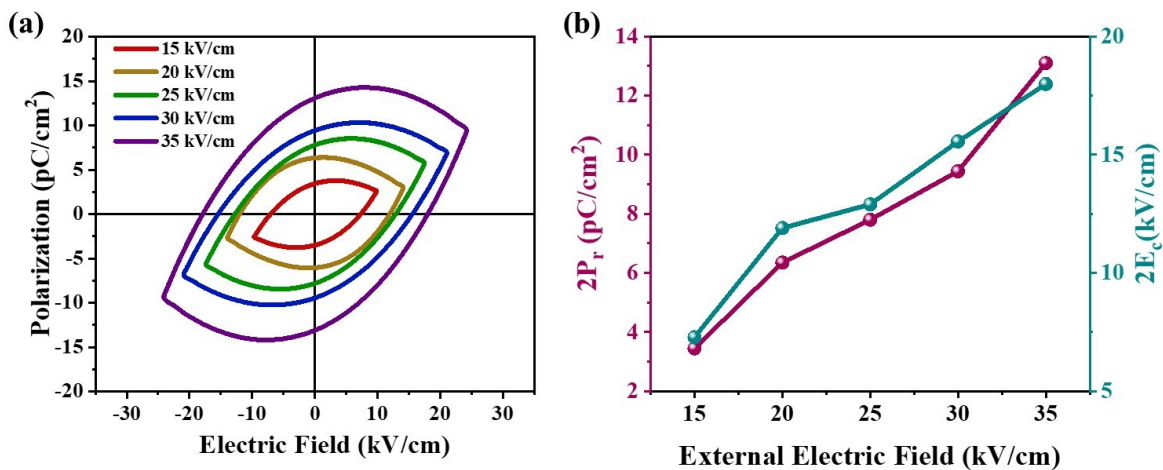


Figure S4: (a) Polarization versus electric field loop of MgFe<sub>2</sub>O<sub>4</sub> and (b) Variation of remnant polarization and coercive field with respect to applied electric field.

The ferroelectric polarization vs electric field (PE) hysteresis loops were plotted for the magnetic nanocomposite film at different external electric fields, viz. 15, 20, 25, 30, and 35 kV/cm, as shown in Figure S4a. The remnant polarization (in terms of 2P<sub>r</sub>) and coercive field (in terms of 2E<sub>c</sub>) values at different electric fields are plotted in Figure S4b. The remnant polarization and coercive field increase approximately linearly with the applied electric field, indicating enhanced domain alignment and switching activity under a stronger field.

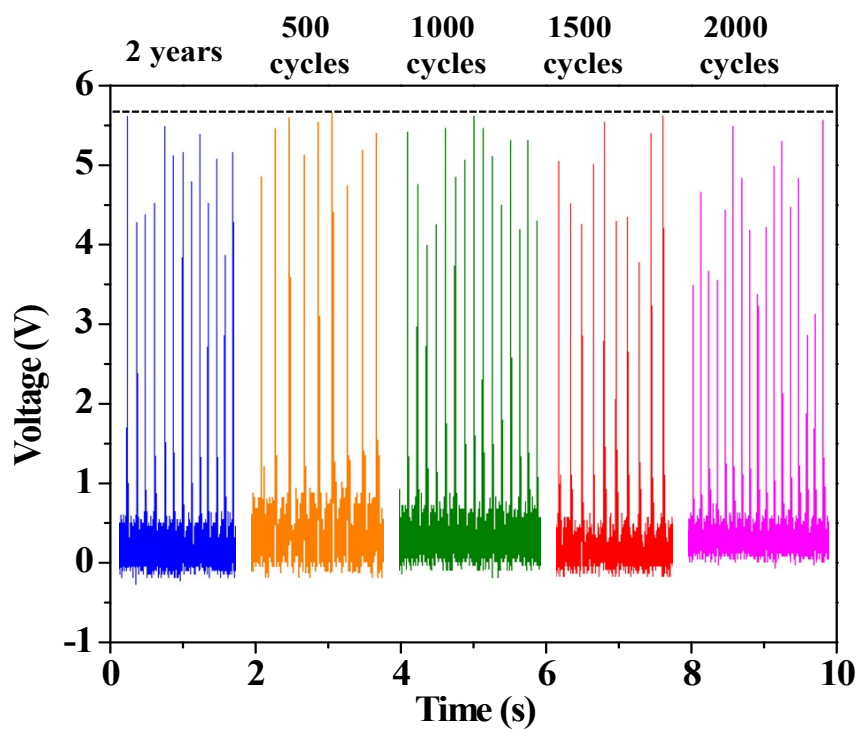


Figure S5: Long-term durability and cyclical stability analysis of the MF-3 nanogenerator under constant force.

To evaluate the long-term durability and cyclic stability, the voltage output of the nanogenerator was tested after two years and for 2000 cycles of mechanical excitation using the stepper motor, as shown in Figure S5. After 2 years of ambient storage and < 2000 cyclic operations, the voltage output is stable (~5.8 V) with slight variations in performance. The excellent electrical response clearly suggests the superior long-term durability, operational stability, and reliability of the nanogenerator.

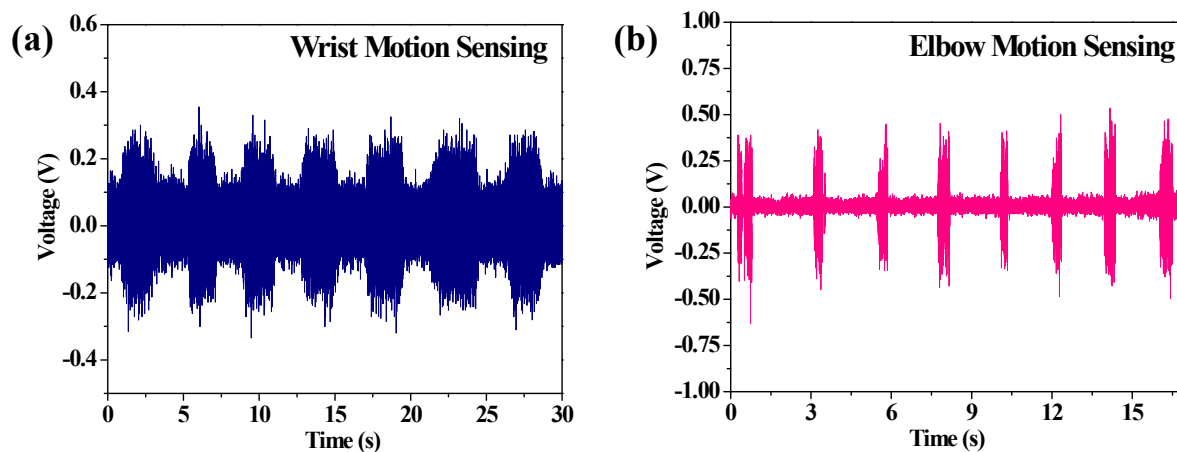


Figure S6: Biomechanical motion sensing of (a) wrist and (b) elbow using MF-3 nanogenerator.

Flexible multifunctional composite materials have been of immense interest for biomedical sensing applications, owing to their high sensitivity to low frequency physiological and biomechanical motions. The ability of the MF-3 nanogenerator for biomechanical motion sensing was demonstrated by attaching the device to different parts of the human body, such as the wrist and elbow, as shown in Figure S6a-b. The nanogenerator generated the specific electrical output signals as a response to the applied mechanical deformation during the bending and relaxation motions, confirming its excellent sensitivity towards human motion. The stable and repeatable voltage response from wrist and elbow movements demonstrates the promising potential applicability of the MF-3 nanogenerator in wearable self-powered motion sensing and human activity monitoring applications.

## References

- 1 Y. Feng, S. Li, Y. Zheng, Z. Yi, Y. He and Y. Xu, *J. Alloys Compd.*, 2017, **699**, 521–525.
- 2 F. Naaz, P. Lahiri, C. Kumari and H. Kumar Dubey, *Phys. Chem. Solid State*, 2023, **24**, 392–402.